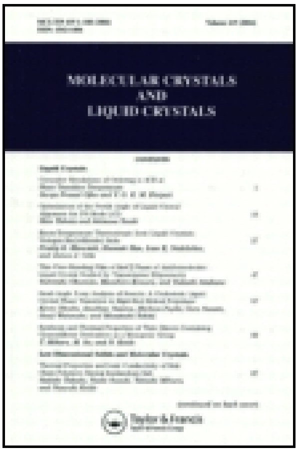

Molecular Crystals and Liquid Crystals Science and Technology. Section A. Molecular Crystals and Liquid Crystals

Publication details, including instructions for authors and subscription information:
http://www.tandfonline.com/loi/gmcl19

Induced Reentrant Smectic A Phase in the Binary Mixtures of Nematic and Cholesteric Compounds

Nagappa [a] , Jagadish. K. N. [a] , Hanumantha Nayak. R. [a] & Siva Prasad. A. [a]

[a] Department of Physics, University of Mysore, Manasagangotri, Mysore, 570 006, INDIA

Version of record first published: 23 Sep 2006.

To cite this article: Nagappa , Jagadish. K. N. , Hanumantha Nayak. R. & Siva Prasad. A. (1995): Induced Reentrant Smectic A Phase in the Binary Mixtures of Nematic and Cholesteric Compounds, Molecular Crystals and Liquid Crystals Science and Technology. Section A. Molecular Crystals and Liquid Crystals, 260:1, 547-564

To link to this article: http://dx.doi.org/10.1080/10587259508038728

Mol. Cryst. Liq. Cryst. 1995, Vol. 260, pp. 547–564
Reprints available directly from the publisher
Photocopying permitted by license only

INDUCED REENTRANT SMECTIC A PHASE IN THE BINARY MIXTURES OF NEMATIC AND CHOLESTERIC COMPOUNDS.

NAGAPPA, JAGADISH. K.N., HANUMANTHA NAYAK. R. AND SIVA PRASAD. A.
Department of Physics, University of Mysore, Manasagangotri, Mysore - 570 006, INDIA.

ABSTRACT The optical studies reveal that binary mixtures of nematic and cholesteric compounds viz., 4(2-2-ethoxy-ethoxy carbonyloxy-cinnamate of 4-hydroxy) 4'-methoxy azobenzol (ACZHM) and Cholesteryl ethyl carbonate (CEC) exhibit cholesteric, smectic and cholesteric phases in the concentration range of the mixture 1 to 9% of CEC, 10 to 40% of CEC and 41 to 99% of CEC respectively. The mixtures with low percentage of CEC exhibit reentrant smectic A - smectic C - smectic A phases. With the help of the phase diagram of binary mixture, the phase behaviour is discussed. The order parameter of the nematic compound ACZHM is estimated. Optical anisotropy of the mixtures is also estimated using density and refractive index data. Numerous optical textures like striped pattern, focal conic, fan shaped and drops are illustrated. Pitch variation with concentration is discussed.

INTRODUCTION

It is well known that when a small concentration of optically active material is mixed in nematic compound, the pitch of the cholesteric increases[1]. Molecular ordering in the cholesteric mesophase may be regarded as equivalent to a twisted nematic structure. Therefore, induced nemato-chiral mixtures are responding for the solution of various scientific problems and for their applications.[2]

In the present investigation we consider the nematic compound 4(2-2-ethoxy-ethoxy carbonyloxy-cinnamate of 4-hydroxy) 4'-methoxy azobenzol (ACZHM) and cholesteryl compound Cholesteryl ethyl carbonate (CEC). The compound CEC exhibits a cholesteric mesophase at room temperature. The basic data of CEC is reported in our earlier paper [3]. In the present work, order parameter of ACZHM and optical textures, optical anisotropy and temperature dependence of the pitch have been studied for induced cholesteric and smectic phases of mixtures of ACZHM and CEC.

EXPERIMENTAL

The chemicals used in this investigation are from M/s. Eastman organic chemicals, USA and Riedal - Dehaenag Seelze - Hannover, Germany and used after purification by recrystallization using Benzene as solvent . The transition temperature T_{N-I} for ACZHM (237.1°C) and T_{ch-I} for CEC (103.2°C) were determined using the polarizing microscope and hot stage. The phase transition temperatures of ACZHM is compared with the values obtained from DSC. The structural formula and transition temperatures are shown in Fig. 1. The differential Scanning Calorimeter (DSC) studies were carried out on Dupont 9000 thermal analyzer with 910 DSC model. The endothermic DSC trace shows two peaks at 84.22°C and 237.72°C which respectively corresponds to solid-nematic and nematic- isotropic transition. The estimated values of enthalpies are 289.25 Kcal/mol and 10.235 Kcal/mol at 84.22°C and 237.72°C respectively.

The density and refractive indices (n_e,n_o) for 5893Å of ACZHM are determined using the technique described in one of our earlier papers [4].

ORDER PARAMETER OF NEMATIC COMPOUND

Using measured values of density and refractive index for 5893 Å at various temperatures, the polarizabilities α_e and

α_o of ACZHM is calculated using Neugebauer and Vuks relations. The values of α_e and α_o are shown in table 1.

Temp. $(T_c - T)$	Neugebauer $\alpha_e/10^{-24}cm^3$	Neugebauer $\alpha_o/10^{-24}cm^3$	Vuks $\alpha_e/10^{-24}cm^3$	Vuks $\alpha_o/10^{-24}cm^3$
12.5	83.2052	57.4601	83.5909	53.384 0
22.5	85.0416	56.5584	87.6696	53.078 9
32.5	87.3966	55.3806	88.2631	52.193 6
42.5	91.1132	54.2509	91.0973	51.875 1
57.5	91.0684	53.5448	93.3873	51.494 0
87.5	93.075	52.5415	99.6246	49.649 9
102.5	94.6426	51.7576	101.9767	48.879 7
127.5	96.4863	50.8358	104.3140	47.767 8
147.5	97.4171	50.3700	104.9659	47.004 5

Table 1. Effective polarizabilities α_e and α_o for ACZHM compound using Neugebauer and Vuks relations.

The orientational order parameter S in the case of nematic liquid crystals is defined through the equation [5]

$$S = [3 \langle \cos^2\theta \rangle - 1] /2. \qquad (1)$$

where θ is the angle between the director and the axis of the rod like molecule. The orientational order parameter may also be expressed in terms of optical anisotropy of the molecule and the effective polarizabilities α_e and α_o of nematic phase as

$$S = (\alpha_e - \alpha_o) / (\alpha_{\parallel} - \alpha_{\perp}) \qquad (2)$$

$\alpha_{\parallel}$ and $\alpha_{\perp}$ being the polarizabilities of the molecule along the long axis and transverse to it respectively.

The optical anisotropy ($\alpha_{\parallel} - \alpha_{\perp}$) of the molecule is estimated using bond polarizability data[6] and Haller plot method[7]. In this method log ($\alpha_e - \alpha_o$) is plotted against log ($T_c - T$). This yields a straight line which is extrapolated upto log T_c. The limiting value of ($\alpha_e - \alpha_o$) is assumed to be the value of ($\alpha_{\parallel} - \alpha_{\perp}$) of the molecule. The experimental values are in good agreement with the values calculated from the bond polarizability data. The order parameter S is calculated at different temperatures using equation 2 and compared with the Maier- Saupe[10] theoretical values in Fig. 2. It is seen that the experimental values of S agree with the Maier - Saupe theoretical values except in the vicinity of the nematic - isotropic transition temperature where the experimental S factors are significantly lower than the theoretical values[11]. This discrepancy may be attributed to the enhanced vibrations of the aliphatic chain of the molecule and more pronounced fluctuations of the director in the vicinity of nematic - isotropic transition. Therefore, the mean field theory is expected to underestimate the temperature variation of S near nematic - isotropic transition.

BINARY MIXTURE STUDIES (Result and discussion)

Mixtures of about ten different concentrations of ACZHM and CEC were prepared by mixing the samples at molten state. In the following the concentrations are defined as the weight percent of CEC in the total weight of the mixture of ACZHM and CEC. It is found that the mixtures of concentration between 1 to 10% CEC, 11 to 55% CEC and 56 to 99% of CEC exhibit cholesteric, induced smectic and cholesteric phases respectively. The phase transition temperatures of these mixtures were measured using polarizing microscope in

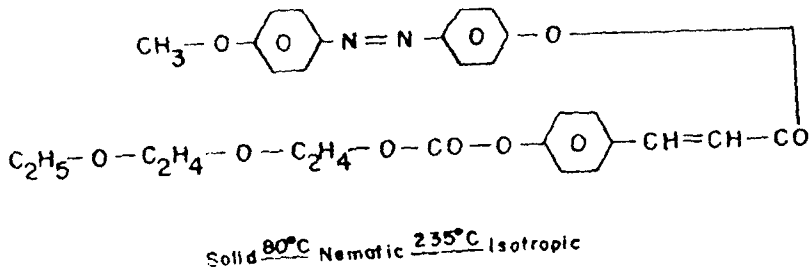

Fig.1. Structural formula of ACZHM

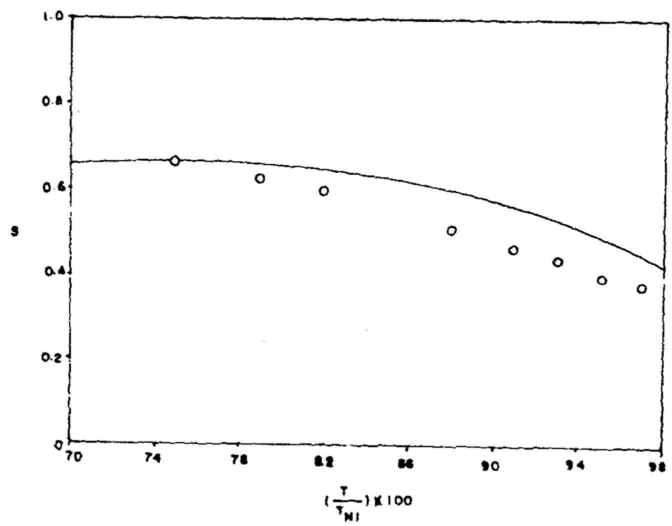

Fig.2. Temperature dependence of S for ACZHM. The solid curve is from Maier-Saupe theoritical values.

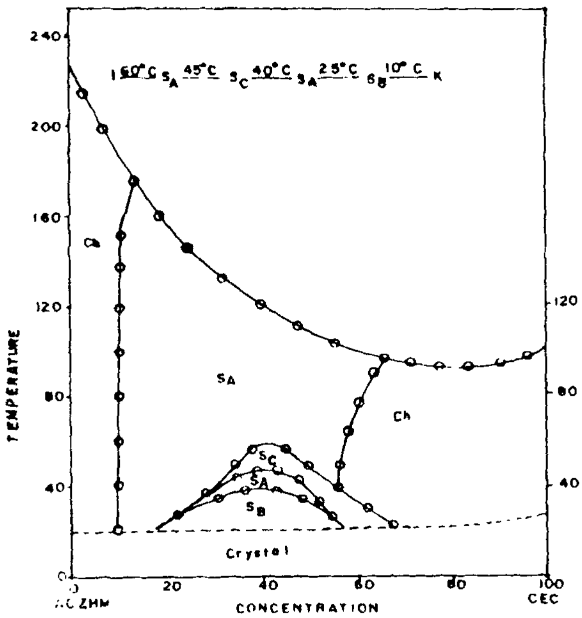

Fig.3. Phase diagram of binary mixture of CEC and ACZHM.

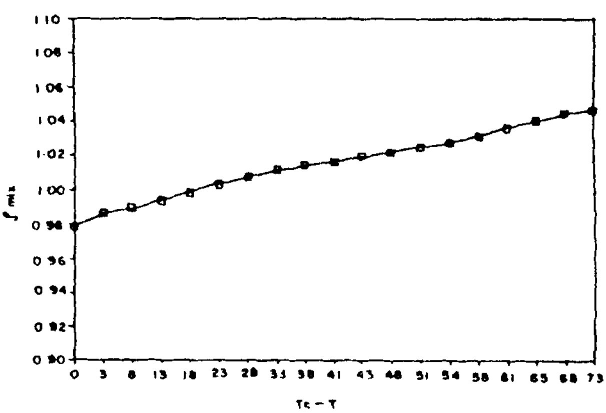

Fig.4. Temperature variation of density of the mixture with 70% concentration of CEC.

conjunction with the hot stage. The samples were sandwitched between slide and cover glass in the form of thin film.

PHASE DIAGRAM

The phase diagram shown[12] in Fig 3 obtained from phase transition temperatures drawn with respect to different concentrations reveals that the concentration range from 1 to 10% of CEC, 11 to 55% of CEC and 56 to 99% of CEC exhibit cholesteric smectic and cholesteric phases respectively. If we cool from isotropic phase, the specimen in the concentration range between 11 to 25% of CEC, exhibits a smectic A phase up to room temperature. In the concentration range between 25 to 55% of CEC the change of phases sequentially follows I- S_A - S_c - S_A - S_B (for 40% CEC) in the temperature range shown in fig 3. The reentrant injected smectic A phase exists between 40 °C to 45 °C while cooling the specimen. The DSC thermogram indicates that the phase change from S_A to S_c is second order.

The samples in the concentration range between 56 to 99% of CEC, when cooled from isotropic phase, exhibit planar texture down to 50 °C and on further cooling the sample crystallises at room temperature.

OPTICAL ANISOTROPY OF THE MIXTURES

The density and refractive indices n_1 and n_2 for 5893 Å in the cholesteric phase of mixtures were measured using Abbe refractometer and precission Goniometer refractometer for different temperatures. The two indices measured here for 55% CEC and above correspond to cholesteric phase. The index n_1 corresponding to the ordinary ray is greater than the refractive index n_2 ($n_1 > n_2$) corresponding to the

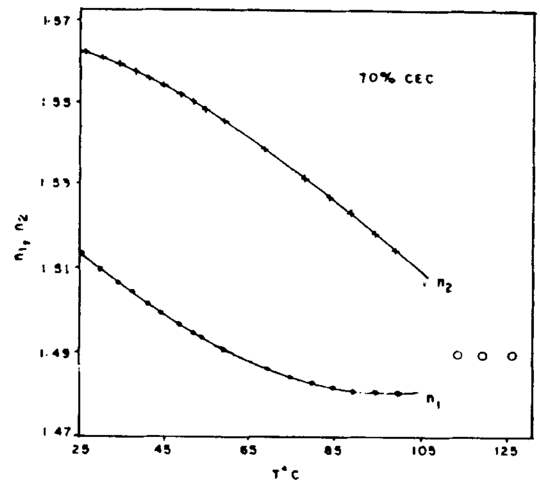

Fig.5. Temperature variation of refractive indices of the mixture with 70% concentration of CEC.

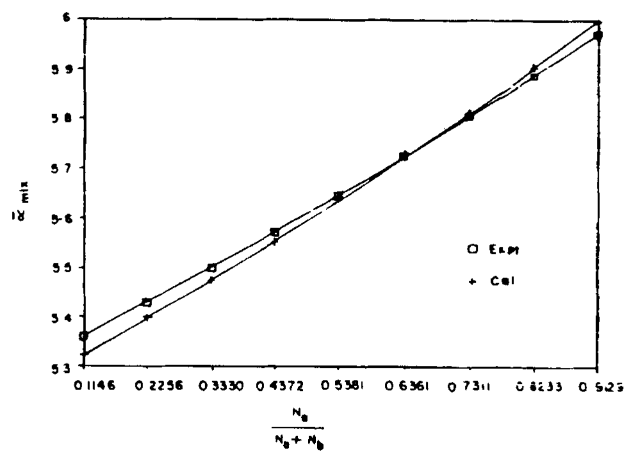

Fig.6. Mean polarizability $\bar{\alpha}_{mix}$ (in units of 10^{-24} cm^3) as a function of N_a/N_a+N_b at a typical temperature of 90.2°C.

extraordinary ray indicating that the material is uniaxial negative being the characteristic of the cholesteric mesophase. It is also possible to measure only one index n_2 in the case of smectic phase exhibited by the concentration between 11 to 55% CEC, n_2 identifiable with ordinary ray in smectic phase. This indicates that the material is uniaxial positive. Temperature variation of density and refractive indices of the mixture with 70% concentration of CEC is shown in fig 4 and 5.

The mean polarizabilities $\bar{\alpha}_{mix}$ of cholesteric phase for different concentrations were calculated using Lorentz -Lorentz relation

$$(\bar{n}^2-1)/(\bar{n}^2+2) = [4\pi/3]\, N(\bar{\alpha}_{mix}) \text{ ---------- } (3)$$

where $\bar{n} = [n_1^2 + 2\, n_2^2]/3$

$$N(\bar{\alpha}_{mix}) = N_a \alpha_a + N_b \alpha_b \text{ and } N = N_a + N_b$$

N_a and N_b are number of molecules per unit volume of CEC and ACZHM respectively and also

$$N_a = (x_a/x_a + x_b)\ (N_A \rho_{mix}/M_a) \text{ ----------- } (4)$$

where M_a is the molecular weight of CEC and N_A is the Avogadro number. Similarly N_b also can be calculated taking M_b as molecular weight of ACZHM, ρ_{mix} is density of mixture.

The effective polarizabilities α_1 and α_2 of cholesteric phase of the mixtures were calculated for ordinary ray n_1 using the relation

$$(n_1^2-1)/(n_1^2+2) = [4\pi/3]\, N(\alpha_1)_{mix} \text{ ---------- } (5)$$

By using correspondingly similar equation for n_2, it is possible to calculate $(\alpha_2)_{mix}$ for the extraordinary ray. The mean polarizability $\bar{\alpha}_{mix}$ is also calculated by

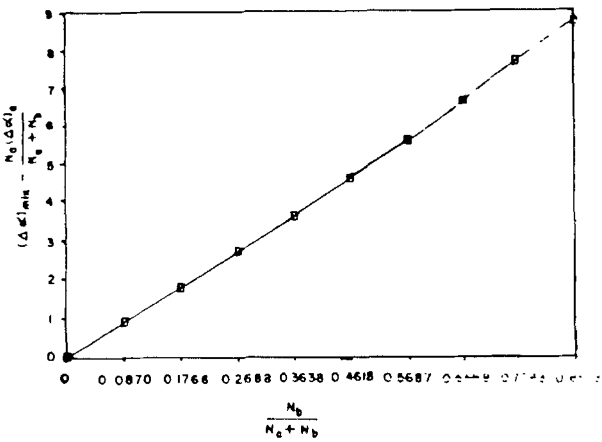

Fig.7. Variation of optical anisotropy of the mixture with concentration. All calculations are made using equation 9 at a typical temperature 90.2°C. The values of $\Delta\alpha$ are in units of 10^{-24} cm^3.

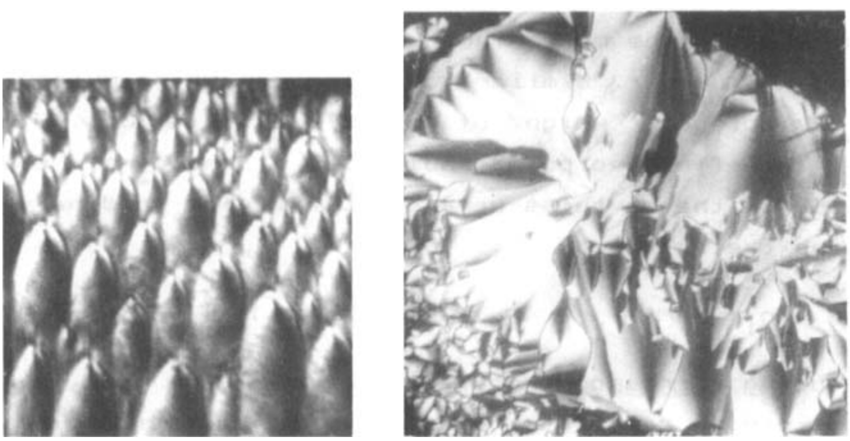

a b

Fig.8. Microphoto'raphs of focal conic textures exhibited by mixtures with crossed polars 500x. a) 35% of CEC b) 40% of CEC.

$$(\bar{\alpha}_{mix})_{expt} = (\alpha_1 + 2\alpha_2)/3 \text{------------} \quad (6)$$

$(\bar{\alpha}_{mix})_{expt}$ values are compared with the values obtained from additivity relation

$$(\bar{\alpha}_{mix})_{cal} = (N_a\alpha_a + N_b\alpha_b)/\ (N_a + N_b) \text{------------} \quad (7)$$

The experimental and calculated values of $\bar{\alpha}_{mix}$ are plotted against $N_a/(N_a+N_b)$ for 90.2°C. Experimental values of $\bar{\alpha}_{mix}$ are in good agreement with the theoretical values shown in Fig. 6.

Further the optical anisotropy of polarizabilities $(\alpha_1-\alpha_2)_{mix} = (\Delta\alpha)_{mix}$ is given by the additivity relation.

$$(\Delta\alpha)_{mix} = [N_a(\Delta\alpha)_a + N_b(\Delta\alpha)_b]/\ (N_a + N_b) \text{----------} \quad (8)$$

$(\Delta\alpha)_a$ and $(\Delta\alpha)_b$ are the anisotropy polarizabilities of CEC and ACZHM respectively. $(\Delta\alpha)_b$ is equal to $(\alpha_e - \alpha_o)$ / 2 at corresponding temperature of the nematic phase and $(\Delta\alpha)_a$ is equal to $(\alpha_1-\alpha_2)$ of CEC. The factor half involved in the expression for $(\Delta\alpha)_b$ arises because the molecules of ACZHM are arranged in the layers of the helicoidal structure of the cholesteric mesophase.

The equation 8 can be written as

$$[(\Delta\alpha)_{mix} - N_a(\Delta\alpha)_a]/(N_a + N_b) = N_b(\Delta\alpha)_b\ /(N_a + N_b) \text{-------} \quad (9)$$

The left hand side of the above equation is plotted against $N_b\ /\ (N_a + N_b)$ in Fig. 7. The slope of the straight line equal to 20×10^{-24} cm^3 is equal to anisotropy of CEC, this being half of the value of $(\alpha_e - \alpha_o)$ 40×10^{-24} cm^3 for ACZHM at 90.2°C.

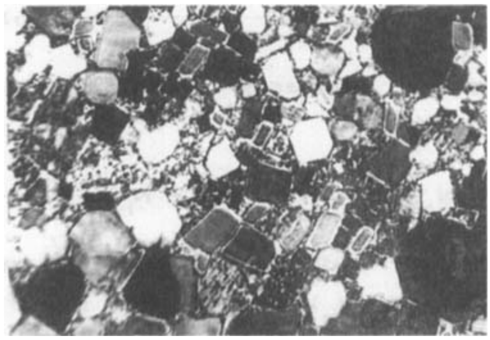

Fig.9. Microphotograph of mosaic texture with 35% of CEC. Crossed polars 185x.

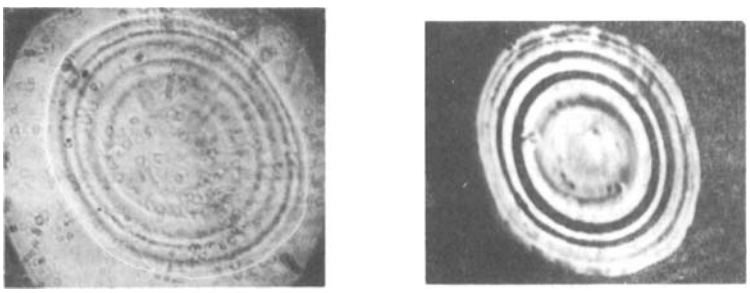

a b

Fig.10. Microphotographs of free cholesteric drop obtained with a specimen having 2% of CEC. a) Using plane polarized white light. Crossed polars120x. b) Using sodium yellow light. Crossed polars 110x.

a b

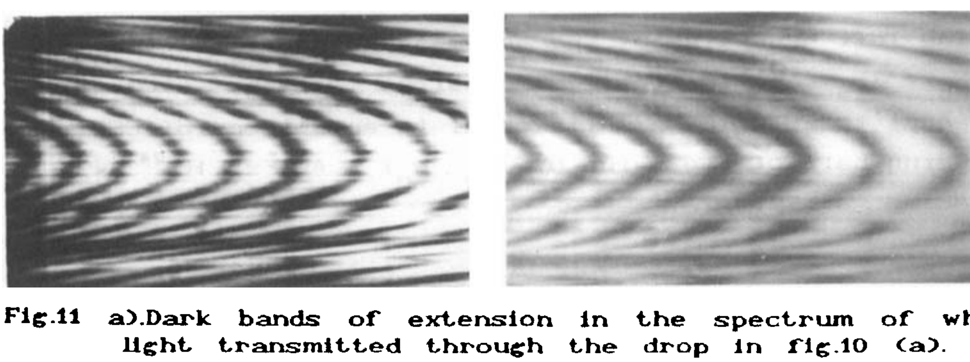

Fig.11 a).Dark bands of extension in the spectrum of white light transmitted through the drop in fig.10 (a). The photograph is obtained with the specimen between the crossed polars. The left hand side of the spectrum corresponds to yellow region in the dark band. The discontinuities occur at the steps. b). With analyser and polarizer in vertical direction.

OPTICAL TEXTURE STUDIES

The cholesteric mesophase frequently encountered with the mixture of low concentration below 10% of CEC and higher concentration between 55 to 99% of CEC exhibits striped pattern and planar texture respectively[13]. The concentrations in the range 11 to 55% of CEC display a rich smectic polymorphism due to the transformation of both the higher temperature smectic textures into lower temperature smectic texture followed by reentrant smectic phase when the sample is cooled from its isotropic melt. The typical focal conic ellipses are shown in Fig. 8 (a) and 8 (b). The X -ray diffraction pattern obtained is characteristic of the smectic A phase. When the mixture of concentrations between 30 to 45% CEC cools from isotropic phase, they straight away exhibit smectic A phase upto 60°C and smectic C phase between the temperature range 45°C to 60°C. In the smectic C Phase the molecules have a tilted arrangement with respect to the smectic layers. The mixture exhibits broken focal conic texture which is the characteristic of smectic C phase. On further cooling, the specimen exhibits reentrant smectic A phase between 45°C to 40°C and then changes to smectic B phase exhibiting mosaic texture shown in Fig. 9.

REENTRANT SMECTIC PHASE

A simple method for obtaining the conventional reentrant smectic phases from strongly deformed conventional or reentrant nematics was investigated by Cladis[14] and others.[15,16]. There are number of pure liquid crystals and liquid crystalline mixtures exhibiting rich smectic polymorphism.[17,18]. Sackman[19] and Demus investigated the novel smectic phases followed by polymorphism.

In most of the cases the conventional and reentrant smectic phases are obtained from strongly deformed nematic reentrant phase[9]. In particular for 40% of CFC the phase changes sequentially as I − $S_A - S_C - S_A - S_B$. usually the reentrant smectic A phase follows reentrant nematic phase. But unfortunately here the reentrant smectic A phase is taking transition from smectic C phase. This may be presumably due to the fact that the mixtures with higher concentration of nematic deforms the sequence of phases[16].

This deformation phase may be responsible for the existance of the reentrant smectic phase. Besides this the other probable reasons for this may be due to intermolecular forces, length of the molecule, rate of cooling, impurity content, super cooling heat flow and temperature distribution, interfacial tension between the low temperature phase sites and the rest of the high temperature phase, surface alignment properties, elastic distortions, energy and pressure changes.[20]

CHOLESTERIC DROPS

Occasionally the cholesteric mesophases exhibit stepped drops with free surface. In these spherical drops a radial molecular arrangement is expected. The typical stepped drop in the cholesteric mesophase is shown in Fig. 10 (a) and 10 (b). Figure 10(a) is obtained using plane polarized light whereas Fig. 10 (b) is photographed with the sample between the crossed polars and yellow light is used in this case. Obviously the drop exhibits dark rings as shown in Fig. 10(b). Each drak ring correspond to a change in optical rotation by an angle π. The textures observed in Fig. 11 (a) and 11 (b) may be explained as follows. When the image of the drop is focussed on the slit of the spectrograph by keeping the drop between the crossed polars and viewed

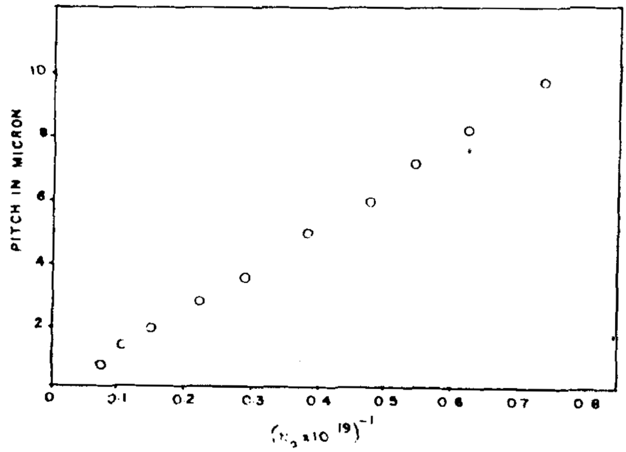

Fig.12. Variation of pitch of the cholesteric mixture with concentration of CEC in the range 0 to 10%. The values of N_a are in the units of 10^{19}/ CC.

through white light the optical rotation can be observed. In the thinner portion of the drop the extinction at lower wavelength are observed. The rotation is larger for the lower wavelengths whereas the extinction shifts to relatively longer wavelengths at the centre of the drop because here the thickness of the drop is large and the same rotation is achieved at the longer wavelengths.

TEMPERATURE DEPENDENCE OF SPIRAL PITCH AND HELICAL TWISTING POWER

Binary mixtures of low concentration of cholesteric in nematic exhibit striped pattern with large pitch. Infact if the pitch is sufficiently large, it is possible to observe under polarizing microscope the stripes associated with helicoidal structure. It is confirmed that there is a periodic variation of the refractive index for the light polarized along the direction of the stripes. Obviously the visibility of the stripes is poor when the incident light is polarized along the direction transverse to the lengh of the stripes.

The pitch of the cholesteric phase is determined by measuring the spacings of the stripes and the angle of diffraction of monochromatic light by the striped texture[21]. It is observed that there is a monotonic increase of pitch with increasing temperature[15].

Fig. 12 illustrates the variation of inverse pitch P^{-1} with the concentration of CEC. Thus a linear dependence of P^{-1} on concentration (C). $P^{-1} = 2AC$ is observed only for small concentration of cholesteric. The A parameter characterizes the helical twisting power value for the mixture for induced cholesteric phase as given in table 2. This result is in confirmity with the rule that for small concentration of cholesteryl compounds in nematics, the pitch should be inversely proportional to the concentration of the cholesteryl compound[13]

Concentration	pitch in μ	$N_a \times 10^{19}$	$A \times 10^3$
1	9.8	1.36	52.02
1.5	6.0	2.0445	55.56
2.5	3.6	3.4079	55.56
5	1.9	6.8175	52.63
6.9	1.4	9.5463	51.76
9	0.8	12.2762	69.44

Table.2. Variation of pitch with concentration

CONCLUSION

Orientational order parameter of ACZHM is estimated using optical anisotropy. Binary mixtures of nematic and cholesteryl compounds exhibit induced smectic phase in addition to cholesteric phase. Lower, higher and intermediate concentrations of cholesteryl material exhibits cholesteric and smectic phases. The polymorphic smectic A, smectic C and smectic B phases are also observed in addition to reentrant smectic A phase. Optical anisotropy in the cholesteric phase of the mixture is also calculated. Beautiful optical textures like fan shaped, drops and striped pattern are illustrated.

REFERENCES

1. Chilaya, Rev. Phys. Appli. **16** 193 (1981)
2. Pavel.J, Glagarova.M, D.Demus, Pelzel.G.Crystal Res. and Technol **18** 915 (1983)
3. Nagappa, D. Revannasiddaiah, Krishnamurti.D Mol .Cryst. Liq. Cryst. **101** 103 (1983)
4. Nagappa, Nataraju.S K ,Krishnamurti.D Mol. Cryst. Liq. Cryst. **133** 31 (1986)
5. Zwetkoff.V Acta. Phys.Chem. USSR **14** (1942)
6. Kahn.F. J Phys. Rev. lett. **24** 209 (1970)
7. Hallar.I, Higgin.H A, Lienthal.H.R and Mequire.I R. Phys.Chem. **77** 950 (1973)
8. Neugebauer.H E. J. Chem Phys. **32** 1 (1954)
9. Vuks.M.F. Opt. Spectrose **20** 361 (1966)
10. Saupe.A and Maier.W. Z. Natur Forsch **16** 816 (1961)
11. Chang. R. Mol. Cryst. Liq. Cryst. **12** 155 (1975)
12. Finn.P L and Cladis. P E. Mol. Cryst. Liq. Cryst. **84** 159 (1982)
13. P.G. de Gennes The Physics of Liquid Cryst. Clavendon press oxford p 219 (1974)
14. P.E. Cladis and S.Torza. J. Appl. Phys **46**, 584 (1975)
15. F.J. Kahn Appl. Phys. lett. **22** 386 (1973)
16. H.P. Hinor and M. Petror Mol. Cryst. Liq. Cryst. **100** 223 (1983)
17. P.A. Gane, A.J. Lead better and P.G. Wrighton Mol. Cryst. Liq. Cryst. **66** 247 (1981)
18. J.C. Dubois Ann. Phys. **3** 131 (1978)
19. H. Sackman and D. Demus Mol. Cryst. Liq. Cryst. **21** 299 (1973)
20. H.P. Hinoo and A.I. Derzhaneki Mol. Cryst. Liq. Cryst. **114** 119 (1984)
21. Nagappa, M. Marthandappa, K.N. Jagadish, A.Siva Prasad, R. Hanumantha Nayak, R. Somashekar and V. Ravindrachary Ind. J. Phys. **68 A (2)**, 151 (1994).